Article

Not peer-reviewed version

An Improved Adaptive Noise Cancellation Algorithm for Interference Suppression in FMCW Radar

Qinmmin Wang *, Chuxiang Chen, Yuming Sun, Wanzhong Sun

Posted Date: 13 April 2026

doi: 10.20944/preprints202604.0862.v1

Keywords: vehicle-mounted FMCW radar; LFM interference; anti-jamming techniques; adaptive noise cancellation; normalized variable step-size LMS algorithm; detection probability

Article

An Improved Adaptive Noise Cancellation Algorithm for Interference Suppression in FMCW Radar

Qinmin Wang [1], Chuxiang Chen [1], Yuming Sun [1] and Wanzhong Sun [2,*]

[1] College of Computer Science, Guangdong University of Science and Technology
[2] School of Marine Science and Technology, Tianjin University
* Correspondence: wqinmin@vip.163.com

Abstract

This study investigates the vulnerability of target signals to co-channel Linear Frequency Modulation (LFM) interference in automotive Frequency-Modulated Continuous-Wave (FMCW) radar systems. It analyzes the limitations of conventional adaptive noise cancellation (ANC) techniques, particularly slow convergence and performance degradation under intense interference. To address these issues, an improved ANC algorithm is proposed. The method generates reference signals through single-channel self-delay processing and adopts a joint optimization framework for weight adaptation, which integrates normalized variable-step-size Least Mean Squares (LMS) adaptation with a leakage factor. Notably, the algorithm achieves robust performance in high-interference scenarios without requiring additional hardware or complex signal transformations. Simulation results verify that the proposed algorithm significantly improves the signal-to-interference-plus-noise ratio (SINR) preserves signal fidelity, and enhances detection probability under strong LFM interference.

Keywords: vehicle-mounted FMCW radar; LFM interference; anti-jamming techniques; adaptive noise cancellation; normalized variable step-size LMS algorithm; detection probability

1. Introduction

Frequency-Modulated Continuous-Wave (FMCW) radar, characterized by its compact structure, low power consumption, high range-measurement accuracy, and strong clutter resistance, is widely used in automotive driving, aerospace, security surveillance, and other fields [1]. The operational performance of this radar directly determines the reliability and stability of the supporting systems. However, with the increasing deployment of vehicular radars, FMCW radar faces growing interference threats, mainly from Linear Frequency Modulation (LFM) [2] and Digital Radio Frequency Memory (DRFM) jamming [3]. The coexistence of these two interferences seriously weakens target echo signals, reducing radar target detection accuracy and anti-jamming robustness. Therefore, developing effective dual-interference suppression methods is of great theoretical significance and practical value.

Domestic and international scholars have conducted extensive research on anti-jamming methods for FMCW radar systems, and a variety of anti-jamming algorithms have been proposed [4]. The Fractional Fourier Transform (FRFT) separates interference and target signals through fractional domain transformation [5], but its suppression effect decreases significantly under strong interference. In contrast, the sparse and low-rank and rankel matrix decomposition for interference mitigation (SPARKLE) algorithm suppresses interference via deramp processing and threshold screening, but it has poor adaptability to dynamic changes in interference parameters [6,7]. Wavelet denoising removes interference components through wavelet decomposition but often causes target signal distortion [8]. The Robust Principal Component Analysis (RPCA) algorithm can effectively separate interference and target signals but cannot meet real-time processing requirements [9].

In comparison, the Adaptive Noise Cancellation (ANC) algorithm is widely used in radar anti-jamming due to its simple structure and good real-time performance. Nevertheless, conventional ANC algorithms are not suitable for complex echo signals and suffer from performance degradation under intense interference [11]. An advanced ANC system is proposed and verified to be feasible in practice, especially in scenarios requiring spatial noise coverage and mitigation of non-ideal operating conditions [12]. ANC shows strong performance in self-interference and noise suppression, with advantages including adaptive tracking of time-varying interference, good real-time performance, simple structure, and easy implementation [13]. However, the ANC algorithm is affected by secondary path modeling errors, frequency mismatch, phase distortion, and non-ideal circuit characteristics. It also faces a trade-off between convergence speed and steady-state accuracy, insufficient suppression of non-stationary or transient interference, and performance degradation in broadband and high-frequency environments.

To address the above challenges, this paper proposes an improved ANC algorithm. First, based on the minimum mean square error (MMSE) criterion and complex signal processing theory, a real-imaginary component separation filtering scheme is designed to solve the error misreporting problem of conventional ANC algorithms in processing complex echo signals. Second, a dynamic step-size adjustment mechanism is developed by estimating the input signal power in real time to optimize the filter coefficient update rule, thus improving the algorithm's adaptability and robustness to dual interferences. Simulation results show that the proposed ANC algorithm has obvious performance advantages, providing a theoretical basis and engineering guidance for dual-interference suppression in FMCW radar systems.

2. System Model

2.1. FMCW Radar Target Echo Model

FMCW radar utilizes a linear frequency modulation scheme, which can be mathematically expressed as:

$$s_t(t)=A_t\exp\left[j2\pi\left(f_ct+\frac{1}{2}kt^2\right)\right] \tag{1}$$

In the equation, A_t represents the amplitude of the transmitted signal, f_c is the carrier frequency and $k=B/T_c$ is the chirp rate where B is the signal bandwidth and T_c is the frequency modulation period.

Assuming a single target exists in the detection range with distance R_t and radial velocity v_t, its echo signal will have time delay $\tau_t=2R_t/c$ (where c is the speed of light) and Doppler frequency shift $f_{dt}=2f_cv_t/c$. For an N_c -channel receiving system, the target echo signal at mth channel can be expressed as:

$$s_{t,m}(t)=A_{t,m}\exp\left[j2\pi\left(f_c(t\text{-}\tau_t)+\frac{1}{2}k(t\text{-}\tau_t)^2+f_{dt}(m\text{-}1)T_c\right)\right]+n(t) \tag{2}$$

In the equation, $A_{t,m}$ represents the echo signal amplitude of the mth channel, n(t) denotes Gaussian white noise, and $(m\text{-}1)T_c$ characterizes the inherent phase differences in multi-channel system.

2.2. Interference Model

This paper investigates anti-jamming for FMCW radar under LFM and DRFM dual interference. The chirp rate of the LFM jamming signal is highly correlated with the radar transmitted signal:

$$s_{lfm,m}(t)=A_{lfm}\exp\left[j2\pi\left(f_c(t-\tau_i)+\frac{1}{2}k_l(t-\tau_i)^2+f_{di}(m-1)T_c\right)\right] \tag{3}$$

 doi:10.20944/preprints202604.0862.v1

In the equation, A_{lfm} denotes the LFM interference amplitude, $\tau_i = 2R_i/c$ (where R_i represents the distance of the LFM interference source), $k_l = k \cdot kl_{factor}$_factor kl_{factor} is a scaling factor for the chirp rate) and $f_{di} = 2f_c v_i/c$ (v_i indicates the radial velocity of the LFM interference source). The intensity of the interference is characterized by the Interference-to-Noise Ratio (INR).

DRFM jamming involves capturing the radar transmitted signal, delaying and amplitude modulating it before retransmission. This process can be mathematically expressed as:

$$s_{drfm,m}(t) = A_{drfm} \exp\left[j2\pi\left(f_c(t - \tau_s - \tau_d) + \frac{1}{2}k(t - \tau_s - \tau_d)^2 + f_{ds}(m-1)T_c\right)\right] \quad (4)$$

In the equation, $A_{drfm} = a_d \cdot A_t$ (where a_d is the amplitude modulation coefficient), $\tau_s = 2R_s/c$ is the round-trip propagation delay from radar to DRFM jammer(R_s is the distance to the DRFM interference source), τ_d is the internal store-and-forward delay of the DRFM jammer (signal capture, quantization, storage, and retransmission delay), and $f_{ds} = 2f_c v_s/c$ (where v_s indicates the radial velocity of the interference source).

2.3. Received Signal Model

The signal received by the radar receiver comprises the target echo, dual interference signals, and Gaussian white noise. This is comprehensively expressed as:

$$s_r(t) = s_t(t) + s_{lfm}(t) + s_{drfm}(t) + n(t) \quad (5)$$

The primary aim of this research is to develop efficient anti-jamming algorithms that can effectively counteract dual jamming signals from LFM and DRFM. This would restore the original properties of target echo signals, thereby improving radar performance in terms of target detection and parameter estimation.

3. Improved ANC Algorithm

The improved ANC algorithm processes the radar composite signal and estimates and suppresses interference in real time through an adaptive filter. The algorithm adopts a real-imaginary separation filtering scheme to correct errors in complex signal filtering and introduces a dynamic step-size optimization mechanism to enhance sensitivity to interference changes. As a result, the system outputs high-purity target echoes with suppressed interference and complete performance indicators, meeting the real-time requirements of radar signal processing.

3.1. Algorithm Structure

The improved ANC algorithm processes the radar composite signal and uses an adaptive filter to estimate and suppress interference in real time. It uses a real-imaginary component separation processing strategy in filtering to correct errors in complex signal processing. In addition, a dynamic step-size optimization mechanism is integrated to improve adaptability to changing interference conditions. Therefore, the system outputs high-purity target echoes with suppressed interference and complete running performance indicators, meeting the real-time requirements of radar signal processing.

The algorithm, which is based on the Minimum Mean Square Error (MMSE) criterion, can be mathematically formulated in the real number domain as follows:

$$\min_w E\left[|e(n)|^2\right] = \min_w E\left[|x(n) - w^T v(n)|^2\right] \quad (6)$$

Here, *e(n)* denotes the error signal, *x(n)* represents the received mixture signal vector, *w* signifies the filter coefficient vector, *v(n)* corresponds to the sliding window input vector, and *E[·]* denotes the mathematical expectation operator. This model can be extended to the complex domain, wherein the error signal is expressed as:

 doi:10.20944/preprints202604.0862.v1

$$e(n)=x(n)-w^{H}v(n) \tag{7}$$

In the equation, H represents the conjugate transpose operation. The improved ANC algorithm comprises six core functional modules, as depicted in Figure 1.

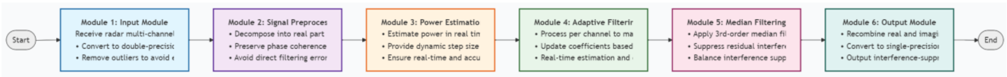

Figure 1. A flowchart illustrating the improved ANC algorithm.

Input Module: This module retrieves the multi-channel complex mixed signal $s_r∈C^{N_s×N_c}$, where N_s represents the number of sampling points, from the radar system. It converts the signal to double-precision floating-point format to improve calculation accuracy, and eliminate outliers to reduce errors in subsequent processing.

Signal Preprocessing Module: The complex mixed signal is decomposed into its real component $Re[s_r]$ and imaginary component $Im[s_r]$. This approach effectively reduces errors associated with direct filtering of complex signals,maintains the phase synchronization of the original signal, and avoids phase distortion.

Power Estimation Module: A sliding average method with a 10-point sliding power estimation is utilized to perform real-time estimation of the input signal power in real time, providing a reliable basis for the dynamic step-size adaptation of the adaptive filter. The window length is matched with the radar sampling frequency to ensure fast response and high estimation accuracy.

Adaptive Filtering Module: This module adopts a per-channel processing framework to match the multi-channel reception requirements of radar systems. Filter coefficients are updated based on the minimum mean square error (MMSE) criterion, integrated with a dynamic step-size strategy to realize real-time estimation and accurate cancellation of LFM and DRFM interferences. As the core of the improved ANC algorithm, this module achieves effective interference suppression.

Median Filtering Module: Apply third-order median filtering separately to the real and imaginary parts of the adaptive filter error signal to further suppress residual interference and noise, while balancing interference suppression effect and target signal retention.

Output Module: Reconstruct the filtered real and imaginary parts into a complex signal, convert it to single-precision floating-point format to reduce memory usage, and the final output comprises the interference-suppressed target echo signal sc, providing key data for algorithm performance evaluation.

3.2. Steps of the Algorithm

The improved ANC algorithm uses a per-channel processing method to match the multi-channel reception characteristics of the radar system. It is fully reproduced in MATLAB simulation code to ensure consistency between theoretical design and practical value implementation. The workflow is as follows:

Parameter Initialization: Configure the adaptive filter order as L=16, the leakage coefficient of 0.9995, and the regularization term $\varepsilon=10^{-6}$. Initialize the filter coefficient vector $w=0_{L×1}$ as a zero vector of dimension $w=0_{L×1}$, and initialize the output signal matrix $s_c=0_{N_s×N_c}$ as a zero matrix of dimension $s_c=0_{N_s×N_c}$.

Signal Preprocessing: Acquire the complex mixed signal s_r received by the radar, decompose it into its real and imaginary components, and set outliers in the signal to zero. This step reduces adverse effects on signal integrity and avoids calculation errors in subsequent processing.

Power Estimation: Perform real-time estimation of the input signal power using $P_{est}=movmean(|s_r|^2,10)$, to ensure the smoothness and real-time performance of power estimation.

Preprints.org (www.preprints.org) | NOT PEER-REVIEWED | Posted: 13 April 2026 doi:10.20944/preprints202604.0862.v1

Per-Channel Adaptive Filtering: Extract the signal of each receiving channel, initialize the error signal vector, use a sliding window to extract the input vector, calculate filter output, error signal, and dynamic step size, then update filter coefficients to achieve real-time interference cancellation.

Median Filtering:Perform third-order median filtering on the real and imaginary parts of the error signal of each channel separately to remove residual interference and noise, then reconstruct the filtered real and imaginary parts into a complex signal.

Result Output: The target echo signal s_c is output following interference suppression.

Exception Handling: Add exception handling logic to limit the filter coefficient range, ensure algorithm stability, be consistent with the exception handling mechanism of the comparison algorithm, and guarantee the fairness of simulation experiments.

4. Simulation Results and Analysis

Simulation Setup

The FMCW radar jamming simulation parameters are set according to automotive radar engineering specifications: a carrier frequency of 77 GHz, bandwidth of 200 MHz, frequency modulation period of 100 μs, chirp rate of 2×10^{12} Hz/s, 16 receiving channels, a target located 50 m away with a velocity of 15 m/s, a signal-to-noise-ratio (SNR) of 15 dB, DRFM jamming INR 18 dB. The LFM jamming INR varies from 10 to 35 dB in steps of 5 dB to test the suppression performance under different interference intensities. Key performance metrics encompass signal-to-interference-plus-noise ratio (SINR) improvement, jamming suppression depth, signal distortion quantified by normalized mean square error(NMSE), and detection probability (DP). As illustrated in Figure 2, the comparative performance curves of anti-jamming algorithms under varying LFM jamming intensities clearly delineate the performance trends of each algorithm as interference levels change.

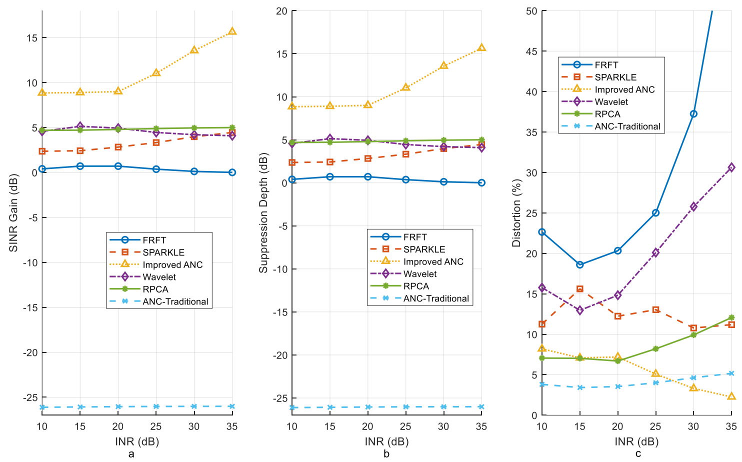

Figure 2. illustrates the performance variation curves of each algorithm in relation to LFM interference intensity. This includes: (a) SINR gain under varying interference intensities, (b) a comparative analysis of interference suppression depth at different interference levels, and (c) signal fidelity across diverse interference intensities.

The figure visually shows the trends of SINR improvement, interference suppression depth, and signal fidelity of the six algorithms with LFM interference intensity. The data clearly show that the improved ANC algorithm outperforms all other algorithms in these three indicators. The algorithm not only has excellent interference suppression ability, but its suppression effect is enhanced with the increase of interference intensity, solving the problem that the conventional ANC algorithm has poor resistance under strong interference. At low interference intensity, the signal fidelity of the improved ANC algorithm is slightly lower than that of the traditional ANC and RPCA algorithms, mainly because the algorithm structure prioritizes robust noise reduction. However, as the interference intensity increases, its advantages become more obvious, and the overall performance is better.

Figure 3 shows the overall average suppression rate of combined LFM and DRFM interference when the LFM interference intensity is 25 dB. The results show that the overall suppression rate of the improved ANC algorithm exceeds 92%, significantly higher than RPCA (68%), wavelet method (64%), and SPARKLE algorithm (54%). In contrast, the traditional ANC and FRFT algorithms have a suppression rate lower than 10%, which is almost ineffective against such dual interference. These results fully verify that the improved ANC algorithm can achieve deep and efficient interference suppression in a strong dual-interference environment, and its comprehensive anti-jamming performance is significantly better than the existing mainstream algorithms.

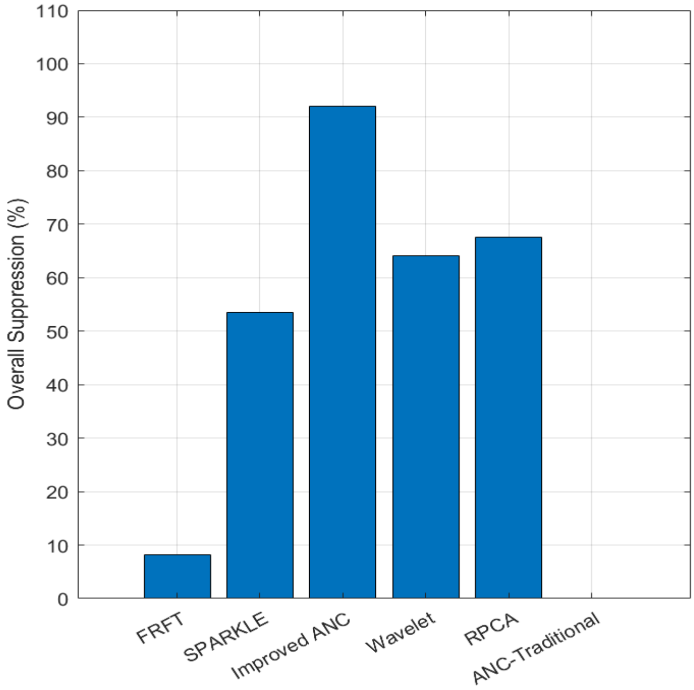

Figure 3. Overall Average Suppression Rate of Combined LFM and DRFM Interference at 25 dB LFM Intensity.

Figure 4 presents a comparative analysis of the output SINR performance across diverse algorithms. As illustrated in Figure 4, the output SINR of each algorithm exhibits a monotonic decline as interference intensity escalates. Notably, the improved ANC algorithm surpasses other algorithms by a margin of at least 10 dB, demonstrating markedly superior noise suppression capability. Through more effective noise attenuation and superior preservation of signal fidelity, the improved ANC algorithm delivers a substantially higher output SINR than its counterparts, thereby establishing its preeminence in comprehensive noise reduction performance.

doi:10.20944/preprints202604.0862.v1

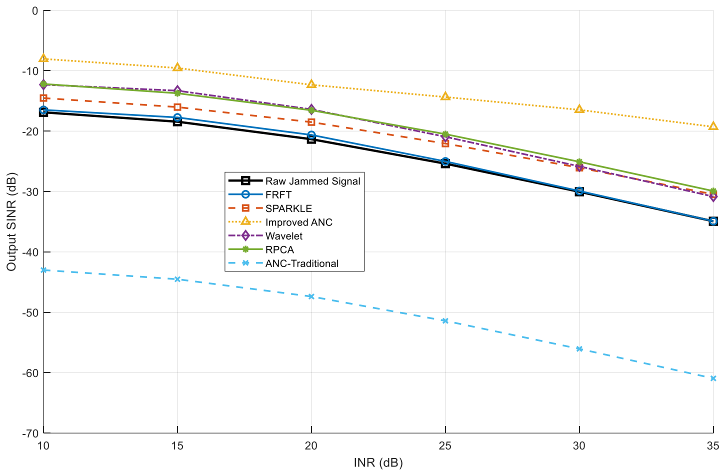

Figure 4. Curves comparing SINR improvement across various algorithms.

Figure 5 shows the detection probability performance comparison curves of different algorithms. As shown in the figure, the improved ANC algorithm is better than other methods in noise suppression depth (INR) and processing efficiency (DP), with a detection probability exceeding 90%. Its detection ability is significantly better than traditional methods and comparison algorithms including wavelet and RPCA. In addition, the algorithm runs efficiently and stably without performance bottlenecks, showing better overall performance and effectively improving the detection probability in complex scenarios.

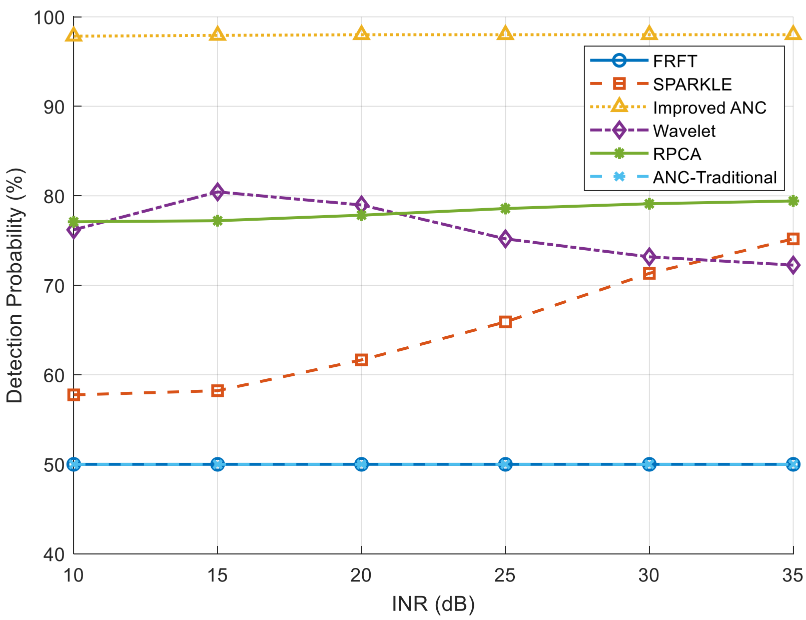

Figure 5. Target detection probability curves as a function of LFM jamming intensity for various algorithms.

The findings indicate that the improved ANC system delivers a suppression level above 92% in the presence of dual interference, secures an SINR improvement of no less than 10 dB relative to comparative baselines, and attains a detection probability exceeding 90% under intense interference conditions.

 doi:10.20944/preprints202604.0862.v1

5. Conclusions

This paper addresses the problem of insufficient interference suppression capability of FMCW radar under the coexistence of LFM and DRFM interferences. An improved ANC is proposed, theoretically derived, and verified by simulation. The main contributions are summarized as follows: the improved ANC algorithm uses real-imaginary decomposition filtering to correct the median filtering error in complex signal processing while maintaining the target phase integrity. A dynamically adjustable step size based on 10-point sliding power estimation and integrated with a leakage factor of 0.9995 is used to balance convergence speed and steady-state error. This significantly reduces the interference-induced degradation of target signals and improves system robustness in a dual-interference environment. The algorithm has a simple structure and good engineering practicability, and is superior to traditional ANC, wavelet, and RPCA methods in interference suppression effect, signal fidelity retention, and system robustness. These advantages provide a reliable anti-jamming scheme for automotive and security FMCW radar applications. Future work will focus on algorithm adaptation to multi-target and complex clutter environments, step-size parameter optimization, experimental verification, and engineering implementation.

Author Contributions: Conceptualization, Wang Qm. and Chen Cx.; Methodology, Chen Cx.; Software, Sun Ym; Validation, Sun Wz.; Formal analysis, Sun Wz.; Investigation, Sun Ym; Resources, ChenCx.; Data curation, Wang Qm; Writing—original draft preparation, Wang Qm; Writing—review and editing, Sun Wz.; Visualization, Sun Wz. Supervision,wangQm; Project administration, Wang Qm; Funding acquisition, Wang Qm.

Data Availability Statement: The data presented in this study are available on request from the corresponding author.

Conflicts of Interest: The authors declare no conflict of interest.

References

1. Pu, W.; Zheng, Z.; Tian, D.; Liang, Z.; Liu, Q. Velocity estimation of DRFM jamming source based on doppler differences in distributed array radar. In Proceedings of the IET Conference Proceedings, 2024; Volume 2023, 47, pp. 387–392.
2. Wang, L.; Liu, M.; Zhang, H. Improvement and simulation of an LFM interference suppression algorithm based on FRFT. Radar Sci. Technol. 2021, 19, 321–327.
3. Kong, Y.; Yu, X.; Li, J.; Cui, G. DRFM-based jamming suppression via convolutional neural network with dilated mechanism. In Proceedings of the 2024 IEEE Radar Conference (RadarConf), 2024; pp. 903–908.
4. Zhang, J.; Han, S. Research on joint interference suppression strategy for vehicle-mounted millimeter-wave radar. SAE Int. 2025. https://doi.org/10.4271/2025-01-8014.
5. Weng, Y.; Chen, G.; Chen, J.; Zhang, Z.; Jia, Z.; Yang, S.; Su, D. FRFT-based interference suppression for automotive FMCW radars. IEEE Trans. Veh. Technol. 2025, 74,pp 8953–8965.
6. Jin, K.H.; Ye, J.C. Sparse and low-rank decomposition of a Hankel structured matrix for impulse noise removal. IEEE Trans. Image Process. 2017, 27,pp 1448–1461.
7. Wang, J.; Ding, M.; Yarovoy, A. Interference mitigation for FMCW radar with sparse and low-rank Hankel matrix decomposition. IEEE Trans. Signal Process. 2022, 70,pp 822–834.
8. Wu, X.-L.; Wang, Z.-Z.; Xi, B.-Q.; Zhen, R. Ground-penetrating radar denoising based on wavelet adaptive thresholding method. IEEE Access 2023, 11,pp 123–135.
9. Kumuda, D.K.; Vandana, G.S.; Pardhasaradhi, B.; et al. Multitarget detection and tracking by mitigating spot jammer attack in 77-GHz mm-wave radars: an experimental evaluation. IEEE Sens. J. 2023, 23, 5345–5361.
10. Ailiya, W.; Yi, W.K.; Varshney, P.K. Adaptation of frequency hopping interval for radar anti-jamming based on reinforcement learning. IEEE Trans. Geosci. Remote Sens. 2023, 61, pp12434–12449.
11. Chen, J.; Li, X.L.; Shen, Y.H.; Lee, S.M. Steady-state performance analysis of the distributed FxLMS algorithm for narrowband ANC system with frequency mismatch. IEEE Signal Process. Lett. 2022, 29, pp1167–1171.

doi:10.20944/preprints202604.0862.v1

12. Wang, H.; Wen, A.; Zhao, C.; Fan, Y.; Peng, M. Photonic-assisted adaptive wideband self-interference cancellation based on self-mixing for FMCW radar. IEEE Trans. Microw. Theory Tech. 2024, 72, pp1–11. https://doi.org/10.1109/TMTT.2024.3505987.
13. Liu, Z.; Boon, C.C.; Yu, X.; et al. A 0.061-mm² 1–11-GHz noise-canceling low-noise amplifier employing active feed forward with simultaneous current and noise reduction. IEEE Trans. Microw. Theory Tech. 2021, 69, pp3093–3106.